ResearchGate

See discussions, stats, and author profiles for this publication at: https://www.researchgate.net/publication/27272158

Influence of Adsorption Conditions on the Structure of Polyelectrolyte Multilayers

ARTICLE *in* LANGMUIR · APRIL 2002

Impact Factor: 4.46 · DOI: 10.1021/la011682m · Source: OAI

CITATIONS
148

READS
33

4 AUTHORS, INCLUDING:

Karlheinz Graf
University Hochschule Niederrhein
50 PUBLICATIONS **1,059** CITATIONS
SEE PROFILE

C. A. Helm
University of Greifswald
124 PUBLICATIONS **4,467** CITATIONS
SEE PROFILE

Available from: C. A. Helm
Retrieved on: 16 January 2016

Influence of Adsorption Conditions on the Structure of Polyelectrolyte Multilayers

Karsten Büscher,[†,‡] Karlheinz Graf,[§] Heiko Ahrens,[†] and Christiane A. Helm*[,†]

Angewandte Physik, Universität Greifswald, Friedrich-Ludwig-Jahn-Str. 16, D-17487 Greifswald, Germany, Institut für Physikalische Chemie, Universität Mainz, Jakob-Welder Weg 11, D-55099 Mainz, Germany, and Institut für Physikalische Chemie II, Universität Siegen, Adolf-Reichwein-Str., D-57068 Siegen, Germany

Received November 16, 2001. In Final Form: January 30, 2002

Polyelectrolyte adsorption onto an oppositely charged interface is determined by electrostatic and secondary interactions. Since polyelectrolytes precipitate at elevated temperatures, the secondary interactions are presumably temperature dependent. This idea is tested for poly(allylamine) hydrochloride/polystyrene sulfonate (PAH/PSS) films adsorbed from aqueous KCl solution (high salt conditions) at temperatures between 5 and 40 °C. KCl was chosen because the films were thicker than those obtained from NaCl or CsCl solutions indicating strong specific binding between K and PSS. The film thickness increases continuously with the adsorption temperature; the changes amount to 20−40%, depending on salt conditions. Furthermore, the roughness is increased, up to a factor of 5. The latter is attributed to the decreased percentage of strong electrostatic bonds within the polyelectrolyte multilayer. Another path to increased roughening is using low-weight polymers with a contour length similar to the thickness of a polycation/polyanion pair.

Introduction

Polyelectrolyte multilayers[1] formed by sequential adsorption of alternating charged polyelectrolytes have been investigated a lot in recent years.[2] With this technique, layered polymeric multicomposites with nanometer control can be built very easily, even on rough or bent surfaces.[3,4] The buildup principle is based on electrostatic interaction; during each adsorption step the surface charge is reversed,[5−7] and thus the adsorption of an oppositely charged polyion is possible again. Yet, the actual surface coverage is also determined by secondary interactions[8] and steric repulsion.[9] The range of possible applications of polyelectrolyte multilayers increased even further when it was realized that not only long-chain molecules but any adsorbed multi-ion such as nanocolloids[10,11] or proteins[12] can be incorporated in a polyelectrolyte multilayer.

However, the adsorption properties of polyelectrolytes are only qualitatively understood. Experimental findings[13,14] and theoretical predictions[15,16] obtained so far may be summarized as follows: Polyelectrolyte adsorption in general is driven by either electrostatic attraction between the polyelectrolyte segments and the surface carrying opposite charges or short-range attractive forces (van der Waals, hydrophobic, hydrogen bonding, or specific forces),[8] leading in most cases to charge reversal. Entropic effects such as counterion release from both the surface and the polyelectrolyte chains[14] also promote polyelectrolyte adsorption. Besides those short-ranged attractive forces, also repulsive forces determine the polyelectrolyte conformation: a multi-ion approaching a surface of the same charge experiences a strong and long-ranged electrostatic repulsion. The polyelectrolyte conformation resulting from this short-ranged attraction and long-ranged repulsion is very flat, corresponding to one or two chain diameters.[14,16] When the substrate with the adsorbed film is removed from the solution, the adsorbed layer remains on the surface because of the pronounced adsorption/desorption hysteresis that is typical for multisegment adsorption.[17] For polyelectrolyte multilayers, the flat, homogeneous adsorption implies a small roughness of the film/air interface, which is very convenient for a controlled polyelectrolyte multilayer architecture.

The flat conformation of adsorbed polyelectrolytes is very different from the coiled conformation (approaching a few radii of gyration) of neutral polymers. For those, the important parameters are polymer length, segment/interface interaction, and the "polymer−solvent interaction parameter w".[18] w is calculated from three inter- and intramolecular interaction energies: solvent−segment (ϵ_{12}), solvent−solvent (ϵ_{11}), and segment−segment (ϵ_{22}).

* To whom correspondence should be addressed. E-mail: christiane.helm@physik.uni-greifswald.de.

† Universität Greifswald.

‡ Universität Mainz.

§ Universität Siegen.

(1) Decher, G. *Science* **1997**, *277*, 1232−1237.

(2) Arys, X.; Jonas, A. M.; Laschewsky, A.; Legas, R. *Supramolecular polyelectrolyte assemblies*; Ciferri, A., Ed.; Marcel Dekker: New York, 1999.

(3) Fou, A. C.; Onitsuka, O.; Ferreira, M.; Rubner, M. F.; Hsieh, B. R. *Mater. Res. Soc. Symp. Proc.* **1995**, *369*, 575−580.

(4) Donath, E.; Walter, D.; Shilov, V. N.; Knippel, E.; Budde, A.; Lowack, K.; Helm, C. A.; Möhwald, H. *Langmuir* **1997**, *13*, 5294−5305.

(5) Lowack, K.; Helm, C. A. *Macromolecules* **1998**, *31*, 823−833.

(6) Bertrand, P.; Jonas, A.; Laschewksy, A.; Legras, R. *Macromol. Rapid Commun.* **2000**, *21*, 319−348.

(7) Schlenoff, J. B.; Dubas, S. T. *Macromolecules* **2001**, *34*, 592−598.

(8) Clark, S. L.; Hammonds, B. *Langmuir* **2000**, *16*, 10206−10214.

(9) Grünewald, T.; Dähne, L.; Helm, C. A. *J. Phys. Chem. B* **1998**, *102*, 4988−4993.

(10) Schmitt, J.; Decher, G.; Dressick, W. J.; Brandow, S. L.; Geer, R. E.; Shashidar, R.; Calvert, J. M. *Adv. Mater.* **1997**, *9*, 61.

(11) Schmitt, J.; Mächtle, P.; Eck, D.; Möhwald, H.; Helm, C. A. *Langmuir* **1999**, *15*, 3256−3266.

(12) Lvov, Y.; Ariga, K.; Ichinose, I.; Kunitake, T. *J. Am. Chem. Soc.* **1995**, *117*, 6117−6123.

(13) Fleer, G. J.; Stuart, M. A. C.; Scheutjens, J. M. H. M.; Cosgrove, T.; Vincent, B. *Polymers at Interfaces*; Chapman and Hall: London, 1993.

(14) Ahrens, H.; Baltes, H.; Schmitt, J.; Möhwald, H.; Helm, C. A. *Macromolecules* **2001**, *34*, 4504−4512.

(15) Joanny, J. F. *Eur. Phys. J. B* **1999**, *9*, 117−122.

(16) Netz, R. R.; Joanny, J.-F. *Macromolecules* **1999**, *32*, 9013−9025.

(17) Cohen-Stuart, M. *Polyelectrolytes on Solid Surfaces*; Daillant, J., Guenoun, P., Marques, C., Muller, P., Vân, J. T. T., Eds.; Editions Frontières: Gif-sur-Yvette, France, 1996; pp 1−12.

(18) Evans, D. F.; Wennerström, H. *The Colloidal Domain*: *Where Physics, Chemistry, Biology, and Technology Meet*; VCH: New York, 1994.

10.1021/la011682m CCC: $22.00 © 2002 American Chemical Society
Published on Web 03/28/2002

Then, $w = \epsilon_{12} - 1/2(\epsilon_{11} - \epsilon_{22})$. For large w, polymer−solvent contact is unfavorable, the chain contracts, and, for very large w, it even precipitates. Theta conditions are characterized by $w = kT/2$, while for $w = 0$ (good solvent conditions) entropy dominates. It is well-known for neutral polymers that on increase of w, more polymer is adsorbed.[13] It would be interesting to see if such a polymer interaction parameter is also relevant for the buildup of polyelectrolyte multilayers.

The polymer−solvent interaction parameter w is determined by short-ranged interactions, extending about a solute diameter. To see its influence on polyelectrolyte adsorption clearly, it is helpful to work with a short-ranged electrostatic interaction, too. The range of the electrostatic interaction is measured by the Debye length, $1/\kappa$, and is a function of the ionic strength. For monovalent ions, the Debye length is given by $1/\kappa = 0.3\ \text{nm}/\sqrt{I}$ (I is the concentration of monovalent salt measured in mol/L).[19] At 1 M salt, the Debye length is equal to $1/\kappa = 0.3$ nm, a value which corresponds to the molecular diameter of water. Polyelectrolyte multilayers can be formed from polyelectrolyte solutions containing that much monovalent salt,[1,20] yet the thickness at each adsorption step exceeds the chain diameter found at low ionic strength by a factor of 3−10. Obviously, at high ionic strength, the adsorbed polyelectrolyte conformation starts to resemble the coiled conformation known from neutral polymers.

Polyelectrolytes are known to precipitate at high temperature,[21] suggesting that the polymer interaction parameter can be gradually increased by adjusting the temperature. To have only short-ranged intermolecular forces, high salt conditions are necessary. High salt concentrations reduce not only the range of the electrostatic force but also the amplitude.[19] Therefore, the balance of forces is drastically shifted. Then, the polymer/solvent interaction parameter is large, and therefore the polyelectrolyte surface coverage should increase. Hence, the study of the temperature dependence appears rewarding.

Materials and Methods

Thoroughly cleaned quartz glass (Crystal GmbH, Berlin, Germany) or silicon wavers (generous gift of Wacker, Burghausen) served as negatively charged substrates. The branched polycation poly(ethylene imine) (PEI, $M_w = 50\,000$, Aldrich) has proved to be an efficient first layer.[22]

The polyanion was polystyrene sulfonate (PSS; PSS, Polymer Standard Service, Mainz, Germany) with five different molecular weights, 350, 168, 83.8, 48.6, and 4.3 kDa (note that the contour length of the shortest polymer is 53 Å, at least a factor of 10 shorter than for all other polymers) with $M_w/M_n \sim 1.1$. The precipitation temperature at high [salt] was found to be 60 °C. For the further buildup of polyelectrolyte multilayers, we used the linear polycation poly(allylamine) hydrochloride (PAH, $M_w = 50-65$ kDa, Aldrich), because of its large flexibility and low persistence length. Ultrapure water was from Millipore (Milli-Q); the salts NaCl, CsCl, and KCl (99%) were from Merck (Darmstadt, Germany).

For each adsorption step during polyelectrolyte multilayer buildup, the substrate was immersed in a 0.003 monomol/L polyelectrolyte (and salt, 1 or 2 M) solution for 30 min and then washed in three beakers of clean water (soaking time, 1 min each). All beakers were kept at the same temperature, which was adjusted externally by a thermostat (Haake, Germany). The films were prepared either by hand (in this case they were dried with a gentle flow of nitrogen before inserting in the UV−vis or X-ray apparatus) or by a robot (Riegler & Kirstein, Berlin, Germany). Except for the 40 °C solution temperature, the mode of preparation had no influence.

UV−vis absorption experiments were performed with a Lambda 900 spectrometer (Perkin-Elmer, U.S.A.; absorption band of the PSS benzene ring at 226 nm).

Specular X-ray reflectivity experiments were performed with a Siemens D-500 powder diffractometer using Cu Kα radiation with a wavelength of $\lambda = 1.54$ Å. The technique provides information on the electron density variation perpendicular to the surface with subnanometer resolution,[23] since the index of refraction depends linearly on the electron density ρ (Thompson radius $r_0 = 2.8 \times 10^{-5}$ Å), $n = 1 - r_0\rho\lambda^2/2\pi$. Since the refractive index is slightly less than 1 (ca. 10^{-5}), dynamic effects (e.g., multiple refraction) contribute only at very small angles of incidence α to the reflected intensity R. Above about twice the critical angle, the reflectivity R (normalized to the Fresnel reflectivity R_F of the ideally smooth surface) can be described by the kinematic approximation[24]

$$\frac{R}{R_F} = \left| \frac{1}{\rho_{sub}} \int_0^\infty \frac{d\rho}{dz} \exp(iq_z z)\, dz \right|^2 \qquad (1)$$

where z is the vertical distance from the substrate surface, ρ_{sub} is the electron density of the substrate (quartz glass or a Si waver), $d\rho/dz$ is the gradient of the electron density along the surface normal, and $q_z = 4\pi \sin\alpha/\lambda$ is the wave vector transfer normal to the surface. Due to the loss of phase information in conventional X-ray reflectometry, the data analysis is based on finding the proper electron density functions, from which the reflectivity is calculated and compared to the measured reflected intensity. The resolution of our instrument was 0.018° corresponding to 0.0026 Å^{-1} determined by a standard slit combination as provided by the manufacturer. For data analysis, any reflectivity curve was first calculated from a model electron density profile and convoluted with this resolution and then compared to the measured reflectivity.

To obtain the optimum interfacial electron density variations, the organic layer is subdivided into homogeneous slabs (box model).[23,24] Each box is parametrized by a length and an electron density. The interfacial roughness is described by an error function of width σ. The roughness has the same effect on the reflected intensity as a Debye−Waller factor; it damps the interference maxima at large q_z. The optimum parameters are determined by a least-squares method.

All polyelectrolyte multilayers prepared below 30 °C could be described very well by one homogeneous slab, with an electron density ρ_1, a thickness $d_1 = d$, and two roughnesses, σ_{sub} for the substrate/film interface and σ_1 for the film/air interface (cf. Table 1). The roughness of the substrate is $\sigma_{sub} = 5-10$ Å (quartz substrates which were subject to multiple cleaning are rougher than new ones or silicon wavers). The electron density profile of polyelectrolyte multilayers prepared at elevated temperatures exhibits a slow and asymmetric decay toward the air (cf. Figure 1). Therefore, more than one box is necessary to describe the experimental data. Yet, various sets of parameters may result in the same electron density profile within the experimental error;[25,26] therefore, for complex models the determination of the parameters is very ambiguous. It is desirable to design a model with as few free parameters as possible.

We chose a second box to describe the large and asymmetrical interfacial roughness (index 2). Please note that the second slab is not correlated with a structural change within the organic thin film. The roughness σ_2 and the thickness d_2 for this slab cannot be determined independently. To avoid any ambiguity,

(19) Israelachvili, J. N. *Intermolecular and Surface Forces*, 2nd ed.; Academic Press: London, 1991.
(20) Schlenoff, J. B.; Li, M. *Ber. Bunsen-Ges. Phys. Chem.* **1996**, *100*, 943−947.
(21) Förster, S.; Schmidt, M. *Adv. Polym. Sci.* **1995**, *120*, 51−133.
(22) Decher, G.; Hong, J. D.; Schmitt, J. *Thin Solid Films* **1992**, *210/211*, 831−835.
(23) Als-Nielsen, J. *Solid and liquid surfaces studied by synchrotron X-ray diffraction*; Blanckenhagen, W. S. a. W., Ed.; Springer: New York, 1986.
(24) Helm, C. A.; Möhwald, H.; Kjaer, K.; Als-Nielsen, J. *Europhys. Lett.* **1987**, *4*, 697−703.
(25) Baltes, H.; Schwendler, M.; Helm, C. A.; Möhwald, H. *J. Colloid Interface Sci.* **1996**, *178*, 135−143.
(26) Tidswell, I. M.; Ocko, B. M.; Pershan, P. S.; Wasserman, S. R.; Whitesides, G. M.; Axe, J. D. *Phys. Rev. B* **1990**, *41*, 1111.

Table 1. Parameters Obtained from the Least Square Fits of the Models Described in the Text to the X-ray Reflectivity Curves[a]

sample[b]	σ_{sub} [Å]	d_1 [Å]	ρ_1 [e$^-$ Å^{-3}]	σ_1 [Å]	d_2 [Å]	ρ_2 [e$^-$ Å^{-3}]	σ_2 [Å]	Γ [e$^-$ Å^{-2}]
PEI[PSS/PAH]$_X$PSS, PSS M_W = 83.8 kDa, 20 °C, 1 M KCl								
2 BL	9.4 ± 0.3	88.0 ± 0.8	0.4	13.6 ± 0.5				33.0
3 BL	14.7 ± 2.1	128.0 ± 3.7	0.4	11.7 ± 0.7				48.1
4 BL	13.4 ± 0.9	161.5 ± 1.4	0.4	9.3 ± 0.3				60.6
5 BL	5.3 ± 0.9	195.3 ± 0.7	0.4 ± 0.1	10.2 ± 0.7				72.1
PEI[PSS/PAH]$_X$PSS, PSS M_W = 83.8 kDa, 20 °C, 2 M KCl								
2 BL	9.9 ± 2.4	116.5 ± 4.1	0.4	14.5 ± 5.1				39.4
3 BL	9.9 ± 2.3	161.8 ± 2.6	0.4 ± 0.2	14.1 ± 2.3				51.6
4 BL	12.9 ± 3.4	235.5 ± 5.4	0.4 ± 0.2	17.1 ± 5.8				73.8
5 BL	6.0 ± 2.6	313.2 ± 2.0	0.3 ± 0.1	11.2 ± 3.7				91.1
PEI[PSS/PAH]$_4$PSS, PSS M_W = 83.8 kDa, 1 M KCl								
5 °C	6.2 ± 0.6	175.3 ± 0.6	0.4 ± 0.1	11.5 ± 0.4				72.2
10 °C	5.1 ± 1.4	180.7 ± 1.1	0.4 ± 0.1	10.6 ± 0.9				71.4
15 °C	6.5 ± 0.6	190.8 ± 0.4	0.4 ± 0.1	10.5 ± 0.4				75.2
20 °C	5.3 ± 0.9	195.3 ± 0.7	0.4 ± 0.1	10.2 ± 0.7				72.1
30 °C	8.3 ± 0.7	32.7 ± 1.4	0.3 ± 0.1	17.3 ± 2.0	202.2 ± 1.4	0.4 ± 0.1	$=\sigma_1$	98.5
40 °C	6.0 ± 0.8	29.5 ± 4.7	0.2 ± 0.4	20.2 ± 1.6	249.9 ± 5.9	0.4 ± 0.1	$=\sigma_1$	103.8
PEI[PSS/PAH]$_4$PSS, PSS M_W = 83.8 kDa, 2 M KCl								
5 °C	9.3 ± 1.0	239.2 ± 3.6	0.4 ± 0.2	12.0 ± 0.60				104.3
10 °C	4.9 ± 0.6	240.5 ± 0.7	0.4 ± 0.1	12.2 ± 0.50				95.5
15 °C	5.0 ± 0.5	257.1 ± 0.5	0.4 ± 0.1	11.7 ± 0.30				101.8
20 °C	4.6 ± 0.4	271.2 ± 1.2	0.4 ± 0.1	15.1 ± 0.60				110.9
30 °C	5.4 ± 0.3	29.8 ± 1.0	0.3 ± 0.1	16.8 ± 2.90	286.7 ± 1.10	0.4 ± 0.1	$=\sigma_1$	113.0
40 °C	4.6 ± 0.7	92.5 ± 33.5	0.2 ± 0.1	52.3 ± 18.9	207.4 ± 27.9	0.4 ± 0.1	$=\sigma_1$	104.6
PEI[PSS/PAH]$_4$PSS, 1 M KCl, 20 °C								
4.3 kDa	6.6 ± 0.5	196.4 ± 0.5	0.4 ± 0.1	22.8 ± 0.5				74.1
48.6 kDa	5.8 ± 0.6	191.1 ± 0.5	0.4 ± 0.1	10.7 ± 0.4				71.3
83.8 kDa	5.3 ± 0.9	195.3 ± 0.7	0.4 ± 0.1	10.2 ± 0.7				72.1
168 kDa	6.2 ± 0.7	202.6 ± 0.5	0.4 ± 0.1	10.4 ± 0.5				79.4
350 kDa	5.8 ± 0.5	208.6 ± 0.5	0.5 ± 0.1	10.7 ± 0.4				83.2
990 kDa	5.9 ± 0.1	196.8 ± 0.8	0.4 ± 0.1	11.0 ± 0.4				58.5
PEI[PSS/PAH]$_X$PSS, PSS M_W = 83.8 kDa, 1 M KCl, 40 °C								
5 BL	7.1 ± 0.5	70.0 ± 14.5	0.3 ± 0.1	27.8 ± 6.2	225.6 ± 15.5	0.4 ± 0.1	$=\sigma_1$	103.9
7 BL	8.5 ± 1.5	54.6 ± 34.6	0.3 ± 0.2	25.7 ± 2.8	488.4 ± 34.3	0.5 ± 0.1	$=\sigma_1$	209.1
10 BL	10.6 ± 0.3	63.8 ± 9.20	0.4 ± 0.1	32.1 ± 15.2	584.5 ± 11.4	0.5	$=\sigma_1$	284.1
15 BL	8.0 ± 0.3	56.0 ± 5.70	0.2 ± 0.1	20.4 ± 3.1	1460 ± 4.40	0.3 ± 0.1	$=\sigma_1$	394.2
PEI[PSS/PAH]$_X$PSS, PSS M_W = 350 kDa, 1 M KCl, 40 °C								
5 BL	7.3 ± 0.4	40.8 ± 8.70	0.3 ± 0.1	22.5 ± 2.3	257.2 ± 9.80	0.4 ± 0.1	$=\sigma_1$	100.8
7 BL	7.3 ± 1.1	32.6 ± 25.3	0.3 ± 0.2	15.6 ± 5.7	488.9 ± 25.3	0.4 ± 0.1	$=\sigma_1$	178.0
10 BL	5.8 ± 0.4	49.8 ± 11.6	0.3 ± 0.1	20.9 ± 2.2	550.5 ± 10.8	0.4 ± 0.1	$=\sigma_1$	202.1
15 BL	6.5 ± 1.0	35.8 ± 17.2	0.2 ± 0.1	18.1 ± 2.4	1318 ± 17.0	0.4 ± 0.1	$=\sigma_1$	465.2
PEI[PSS/PAH]$_X$PSS, PSS M_W = 990 kDa, 1 M KCl, 40 °C								
5 BL	9.4 ± 0.6	39.5 ± 7.30	0.3 ± 0.1	21.5 ± 1.6	231.6 ± 7.40	0.5 ± 0.1	$=\sigma_1$	110.4
7 BL	9.5 ± 1.5	69.7 ± 26.2	0.4 ± 0.1	24.8 ± 7.8	388.1 ± 27.0	0.5 ± 0.1	$=\sigma_1$	182.5
10 BL	6.5 ± 0.6	50.0 ± 9.90	0.3 ± 0.1	18.5 ± 1.3	551.1 ± 8.60	0.4 ± 0.1	$=\sigma_1$	204.8
15 BL	8.6 ± 3.3	30.2 ± 11.3	0.2 ± 0.1	13.6 ± 2.1	1145 ± 21.5	0.4 ± 0.2	$=\sigma_1$	414.7
PEI[PSS/PAH]$_X$PSS, PSS M_W = 83.8 kDa, 20 °C, 1 M CsCl								
2 BL	5.7 ± 0.6	85.9 ± 0.7	0.4 ± 0.1	11.7 ± 0.6				33.5
3 BL	8.9 ± 1.0	121.0 ± 1.5	0.5 ± 0.1	15.9 ± 1.1				55.3
4 BL	5.8 ± 0.9	157.3 ± 0.8	0.5 ± 0.1	12.4 ± 0.6				70.5
5 BL	5.8 ± 0.7	194.3 ± 0.8	0.5 ± 0.1	12.6 ± 0.5				84.1
PEI[PSS/PAH]$_X$PSS, PSS M_W = 83.8 kDa, 20 °C, 2 M CsCl								
2 BL	4.3 ± 0.4	92.9	0.4	11.2 ± 0.7				36.6
3 BL	5.6 ± 0.1	128.8	0.4	12.5 ± 0.3				55.6
4 BL	8.6 ± 0.6	171.5	0.4	15.8 ± 2.0				74.1
5 BL	4.9 ± 0.3	210.4	0.4	11.0 ± 0.5				90.9

[a] The error of each parameter was determined by varying it systematically (while simultaneously adjusting all other parameters to minimize χ^2), until χ^2 was increased by 30%. The large errors in the electron density are probably an effect of the less than ideal footprint correction. [b] BL = bilayers.

a constraint $\sigma_1 = \sigma_2$ was introduced to the model.[27] The thickness of the film is $d = d_1 + d_2$. Obviously, with a different function to describe the profile (Gaussian, parabolic[25]), we would have obtained different values for σ_1 and σ_2. These parameters are useful to monitor changes of the film, yet to compare the X-ray reflectivity results with those obtained by other methods, one needs model-independent parameters. One such parameter is the electronic surface coverage, $\Gamma = \int \rho_{film}(z)\, dz$. In the case of a smooth film with constant electron density (modeled by one box), the integral simplifies to $\Gamma = \rho_1 d_1$.

To explain that approach, we show the electron density profile $\rho_{film}(z)$ and its gradient, $d\rho_{film}(z)/dz$, of the roughest prepared films (5 bilayers, T = 40 °C, adsorbed from 2 M KCl) in Figure 1. As eq 1 shows, X-rays are reflected when the electron density profile changes. We describe the film with slabs, the interface smeared with an error function. The gradient of an error function is a Gauss function, and its full width at half-maximum (FWHM) is

(27) Asmussen, A.; Riegler, H. *J. Chem. Phys.* **1996**, *104*, 8159−8164.

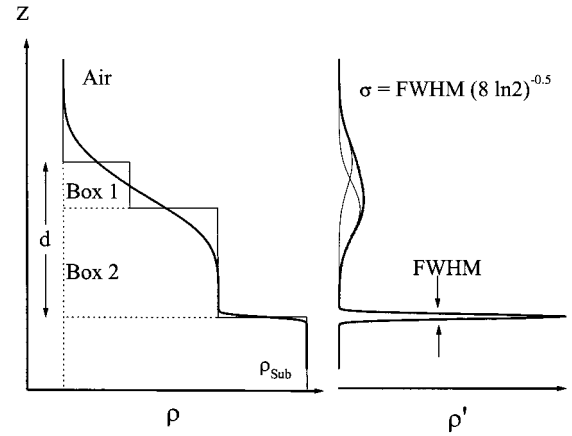

Figure 1. Schematic of the slab model developed for very rough films: Electron density profile $\rho_{film}(z)$ and its gradient, $d\rho_{film}(z)/dz$, of one of the roughest films prepared (5 bilayers, $T = 40$ °C, adsorbed from 2 M KCl). The interfacial roughness is described by an error function. The gradient of this function is a Gauss peak. While the substrate/film interface (in our model, substrate/box$_2$ interface) can be unambiguously modeled with one error function, the slow decay of the electron density toward the air is approximated by two overlapping error functions, with the additional constraint $\sigma_1 = \sigma_2$.

correlated with the roughness σ according to σ = FWHM/$(8 \ln 2)^{1/2}$. While the substrate/film interface (within our model, it is the substrate/box$_2$ interface) can be unambiguously modeled with one error function, we found no analytical function to describe the slow decrease of the electron density toward the air. We used two overlapping error functions with the same width $\sigma_1 = \sigma_2$ to approximate this decay.

Results

We want the monomer/solvent interaction to strongly influence polyelectrolyte surface coverage; therefore, we need small and short-ranged electrostatic forces. This can be achieved with high salt concentrations. First of all, the influence of different monovalent salts in the adsorption solution of PEI(PSS/PAH)$_X$PSS layers is investigated. The thickness and electron density of the films was determined with X-ray reflectivity, and it is found that both the film thickness and the surface coverage Γ increase linearly with the number of adsorption cycles for all types of salts. However, the increment is salt dependent.

Adsorption from KCl solutions leads to thicker films, at least 10% compared to NaCl or CsCl. The same ion specificity is found for 1 and 2 M salt, even though the quantitative values differ (Figure 2a). As shown in Figure 2b, at 2 M KCl the thickness increase per polycation/polyanion layer pair is 61.2 Å, almost an order of magnitude larger than for a layer pair adsorbed from a salt-free solution (~6.5 Å).[28]

Since the original surface charge is over-compensated on polyelectrolyte adsorption, more polymer material is

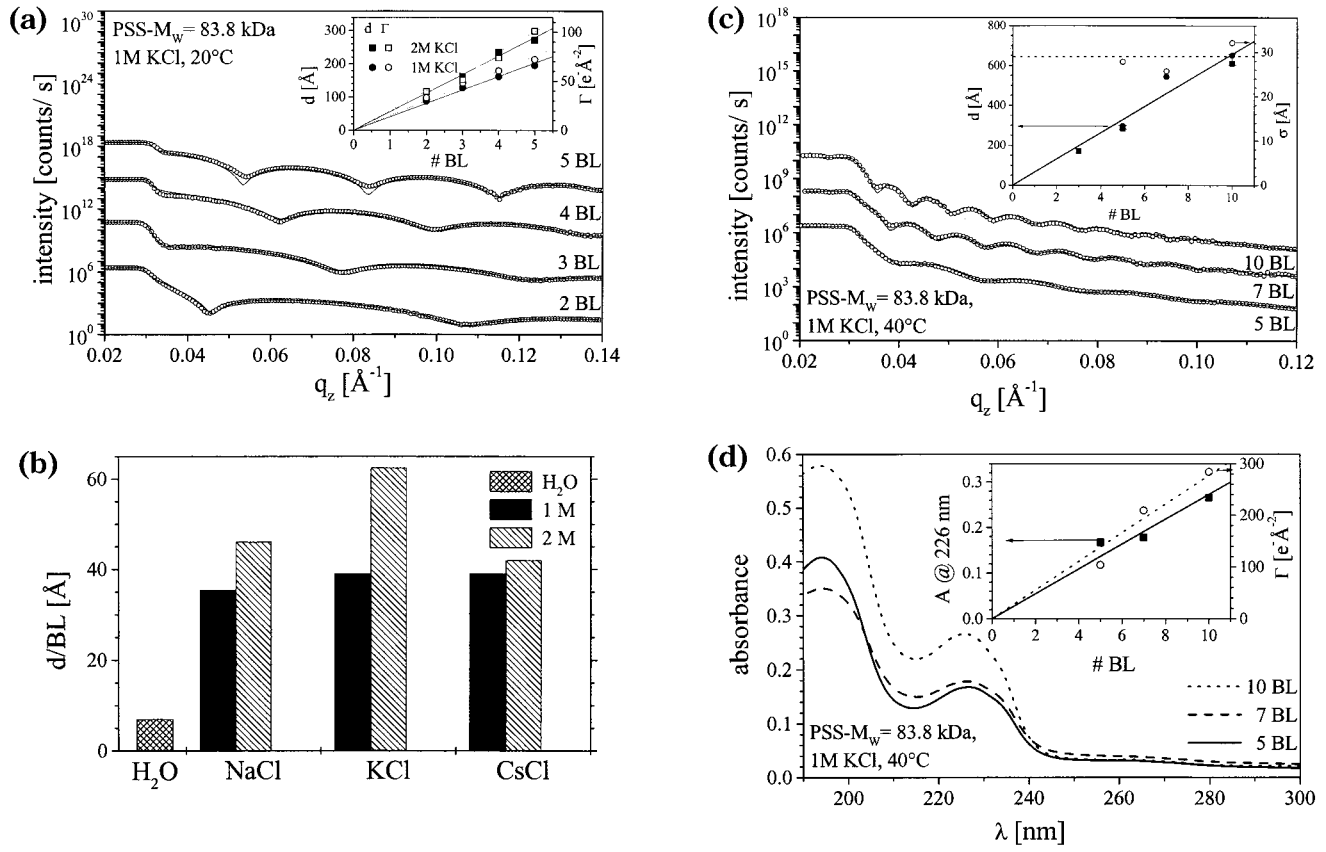

Figure 2. Multilayer buildup at 20 °C (a and b) and at 40 °C (c and d). (a) X-ray reflectivity curves monitoring the multilayer buildup PEI(PSS/PAH)$_X$PSS at 1 M KCl solution and 20 °C (M_w(PSS) = 83.8 kDa). For clarity, the X-ray reflectivity curves are shifted relative to each other. Inset: Dependence of film thickness and coverage $\Gamma = \int \rho_{film}(z)\, dz$ on the number of polyanion/polycation bilayers. (b) Thickness increase per polyanion/polycation bilayer (BL) at solution conditions indicated, $T = 20$ °C. For comparison, data for NaCl and pure water from the literature are shown (ref 28). (c) X-ray reflectivity curves monitoring the automatic multilayer buildup (which was found to produce the smoothest films) at the same conditions as in (a), but at an elevated solution temperature of 40 °C. Inset: Dependence of film thickness and film/air roughness σ on the number of polycation/polyanion bilayers. (d) UV−vis absorption spectra of polyelectrolyte multilayers after 5, 7, and 10 adsorption cycles at a solution temperature of 40 °C. In the inset, the absorbance at 226 nm for the different films is shown (solid symbols), together with the coverage determined from X-ray reflectivity, $\Gamma = \int \rho_{film}(z)\, dz$ (open symbols). The lines are guides to the eye.

adsorbed if the polymer is weakly charged. It seems that the chain charge of PSS is reduced in KCl solution, suggesting a stronger binding of K^+. Precipitation occurs in 1 M KCl solution at 60 °C. Up to a solution temperature of 40 °C, it is still possible to build multilayers (cf. Figure 2c). Again, both the film thickness and the surface coverage Γ (data not shown) increase linearly with the number of adsorption cycles. However, the film/air roughness is increased: a two-box model is necessary, with an increased roughness parameter σ of about 30 Å (instead of 10 Å at room temperature). The average thickness of a polyanion/polycation bilayer is 67.6 Å, a 70% increase compared to 20 °C (39.1 Å). However, at elevated temperatures the multilayer buildup is less robust. At 20 °C, we did the dipping and washing steps both manually and automatically. Sometimes, the samples were dried with a gentle flow of nitrogen. All these variations had no measurable effect. However, at 40 °C, preparation by hand leads generally to rougher films. Drying with nitrogen could increase the roughness parameter to values as high as 50 Å. Apparently, the top polyelectrolyte layer is bound by weak forces; it deforms easily.

UV−vis absorption spectra monitoring the benzene absorption maximum at 226 nm also indicate continuous multilayer buildup (Figure 2d), even though the dependence on sample preparation is even more pronounced than the one found for the film/air roughness. The relationship of benzene absorption to film thickness is a measure for the monomer ratio polycation/polyanion, which can be changed by specific ion binding between the PAH and PSS monomer units.[27,28] According to the literature, all multilayers prepared from various NaCl solutions exhibit a ratio between the absorbance at 226 nm and the film thickness of $E_{226}/d = 6 \times 10^{-4}$/Å (±5%), whereas for adsorption from clean water this value is reduced by a factor of 2 (3.4×10^{-4}/Å). The difference is attributed to the more flat conformation of the PSS chain, if adsorbed from no salt. (The benzene rings of the PSS contribute to the adsorption only if they are aligned parallel to the substrate normal. Relative to the polymer backbone, the benzene rings are tilted.[4] Thus, changing the polymer backbone orientation from parallel to perpendicular, relative to the substrate surface, increases the absorption from almost zero to maximum, and slight changes in the chain conformation may lead to major changes of the absorbance.) The ratio E_{226}/d was always found to be independent from the number of adsorption cycles. This is different for the films prepared from KCl solutions at 40 °C. Also, as mentioned above, E_{226} increases roughly linearly with the number of adsorption cycles, yet at 40 °C, after 10 adsorption cycles the ratio E_{226}/d decreases to half of the original value. This subtle effect is another indication that the binding of the polyelectrolytes to the surfaces is caused not only by electrostatic but also by secondary forces (hydrophobic or van der Waals).

The effect of the adsorption solution temperature is explored systematically in Figure 3a for PEI(PSS/PAH)$_4$PSS layers. Considering the X-ray reflectivity curves, two effects are obvious. With increasing adsorption temperature, the interference minima shift to lower q_z indicating film thickening. The thinnest films are prepared from 5 °C solutions. Thickening gets stronger at 30 °C and even more so at 40 °C; simultaneously, the contrast between maxima and minima disappears with increasing q_z, an effect which indicates a roughening of the film/air

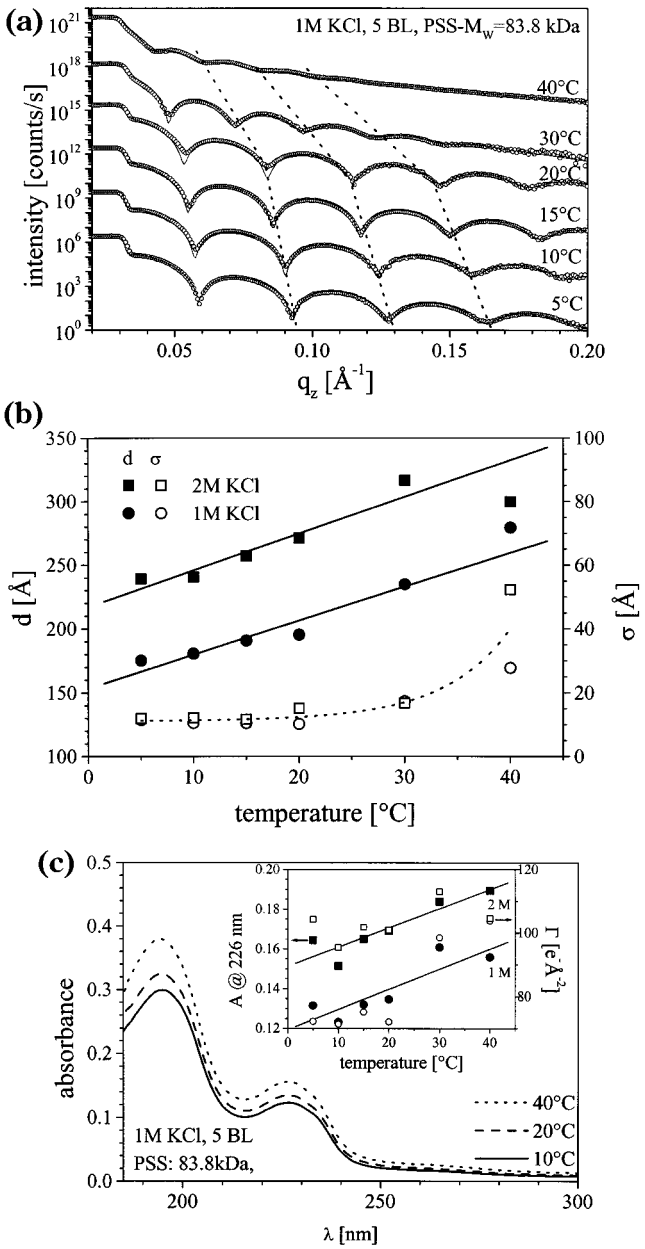

Figure 3. (a) X-ray reflectivity curves of PEI(PSS/PAH)$_4$PSS films prepared from 1 M KCl (PSS M_w = 83.3 kDa) solution at different temperatures. For clarity, the X-ray reflectivity curves are shifted relative to each other; the lines connecting the minima are guides to the eye. (b) The film thickness (solid symbols) and the roughness (open symbols) as functions of the solution temperature, both for adsorption steps with 1 M KCl (squares) and 2 M KCl (circles). (c) Representative UV−vis adsorption spectra at different temperatures. In the inset, the absorbance at 226 nm for the different films is shown (solid symbols), together with the coverage determined from X-ray reflectivity, $\Gamma = \int \rho_{film}(z)\,dz$ (open symbols). The lines are guides to the eye and are not inspired by any theoretical model.

interface (cf. Figure 3b). The thickness is increased by 40% (1 M KCl) or 20% (2 M KCl). The surface roughness is constant up to 20 °C solution temperature, and then it increases dramatically.

An increase in film coverage with temperature is also found with UV−vis absorption spectroscopy (cf. Figure 3c), even though there is considerable scatter in the data. For the films depicted in Figure 3, we found $E_{226}/d = 6.4 \times 10^{-4}$/Å (±5%), independent of solution temperature or ionic strength. However, for temperatures above 30 °C this constant value is probably a coincidence, since the

(28) Schmitt, J. *Aufbau und strukturelle Charakterisierung von Multilagen aus Polyelektrolyten, Reaktivpolymeren und Kolloiden*; Johannes Gutenberg-Universität: Mainz, Germany, 1996.

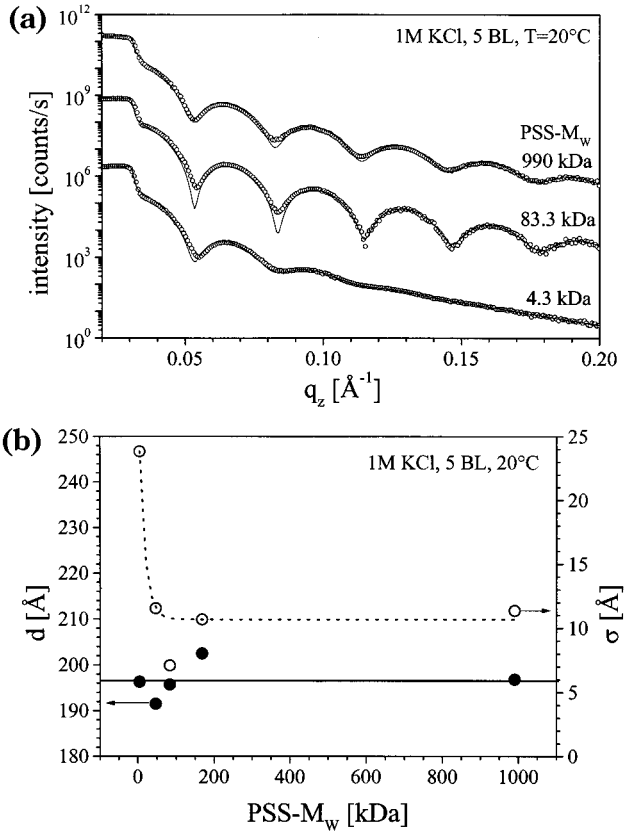

Figure 4. (a) Representative X-ray reflectivity curves of PEI-(PSS/PAH)$_4$PSS films prepared from 1 M KCl solution at 20 °C with different molecular weight PSS (4.3, 83.3, and 990 kDa) and (b) the film thickness and film/air roughness as functions of the PSS weight. The lines are guides to the eye.

absorbance E_{226} is not directly proportional to the coverage. To obtain the surface coverage from X-ray analysis, one has to use the fitted electron density, which exhibits the largest error bars, resulting in uncertainties. The coverage as determined from X-ray reflectivity changes by 40% (1 M KCl) or 15% (2 M KCl). The changes of absorbance are less or comparable, 22% (1 M KCl) or 19% (2 M KCl). X-ray reflectivity and UV−vis absorption experiments yield the same qualitative trends, even though they monitor different physical parameters.

The strong influence of the solution temperature on film thickness and roughness suggests that polymer molecular weight[13] may become important, too. To address that question, a solution temperature of 20 °C was chosen, since the solvent quality is already decreasing, yet the air/film roughness is still small (cf. Figure 4). For polymer molecular weights exceeding 83.3 kDa, we find constant film thickness and roughness. However, the film with the shortest polymer (M_w = 4300 D) exhibits a large film/air roughness (23 Å). That makes sense, if one realizes that the contour length of that polymer, 52.5 Å, is almost identical to the persistence length of neutral polystyrene, 50 Å,[21] and of the same order of magnitude as the thickness per layer pair (39 Å). Adsorption of arbitrarily oriented sticks leads to a rough film/air interface. However, if the polymer molecular weight is increased by a factor of 10, the stratifying effect expected from polyelectrolyte adsorption can be found again, indicating that still electrostatic forces dominate.

Discussion

Our original concept worked; that is, the increasing polymer−solvent interaction causes an increase of the adsorbed amount of polyelectrolyte. This was realized by focusing on short-ranged interactions (reducing the range of the electrostatic interactions by ions) and approaching the precipitation temperature.

We could achieve the same thickness per adsorption cycle either by increasing the ionic strength or by increasing the adsorption temperature. At 2 M KCl and 20 °C, the thickness increase per adsorption cycle corresponds to the values found at 1 M KCl and 40 °C. Yet, there are qualitative changes within the film which we did not expect. The UV−vis experiments show that at elevated temperature the ratio PAH/PSS and/or the PSS chain orientation is no longer the same for each adsorption cycle. An increased dependence of the multilayer buildup on the details of the preparation process is observed, as well as a pronounced roughening of the film/air interface. These features suggest an increased lateral inhomogeneity of the polyelectrolyte multilayers.

Ion specificity was investigated. The thickest films are obtained when adsorbed from KCl solutions, compared to NaCl or CsCl. Since the size of the K^+ is intermediate, cation size effects are not dominant. Note that monovalent ions are never found in polyelectrolyte multilayers;[29] any bound counterions are removed during the three washing cycles following each adsorption step. Yet, the polyelectrolyte/counterion binding constant exhibits ion specificity.[21] Specific binding of the cation to the polyelectrolyte leads to a reduced polymer charge. This necessitates the adsorption of more polyelectrolyte to over-compensate the surface charge. However, the salt and its concentration are only important during the adsorption process; the monovalent salt is removed during the washing. Therefore, we conclude that the ion specificity can be attributed to the binding constant between PSS and the counterions.

To explain the roughening, it is necessary to consider the forces determining the adsorption thickness at high salt concentrations.[16] At good solvent conditions, there is a well-defined amount of adsorbed polyelectrolyte, even if the polymer/solvent interface is very rough.[14] On drying, the adsorbed polyelectrolyte layer collapses onto the solid support and forms a layer with a very homogeneous thickness. Considering the short-ranged yet very large attractive forces found in surface forces experiments,[5] the strong bonds immobilizing an additional polyelectrolyte monolayer to the oppositely charged polyelectrolyte multilayer are local ion bonds between cationic and anionic monomers. Furthermore, in the surface forces experiments the attractive forces were found to be independent of the salt concentration in the solution. These ionic bonds are extremely strong; however, they are thought to be very local, since they depend on the exact monomer position and orientation. Therefore, only a part of the monomer groups are involved in pinning the newly adsorbed polymer to the existing polyelectrolyte multilayer.

In contrast, neutral polymers are adsorbed by many weak bonds.[13] Actually, the thickness of the adsorbed layer can be correlated with the polymer molecular weight, and the bound polymer coil is subject to very little deformation. We find no influence of polymer length indicating still a dominant role of the strong electrostatic forces. However, due to the weak polymer/surface interaction forces, neutral adsorbed polymers are very susceptible to desorption, lateral movement, and so forth, all effects which easily cause lateral inhomogenity and thus increased roughness. These results are consistent with our findings at elevated temperatures. Apparently, more weak bonds due to

(29) Schlenoff, J. B.; Ly, H.; Li, M. *J. Am. Chem. Soc.* **1998**, *120*, 7626−7634.

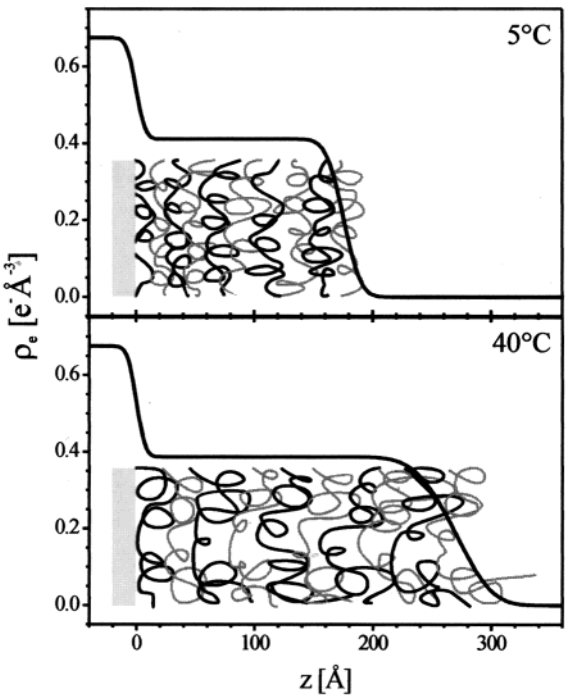

Figure 5. Electron density profiles together with a schematic of the polyelectrolyte multilayer showing less contact between oppositely charged chains as deduced from the top and bottom X-ray reflectivity curves shown in Figure 3a.

secondary interactions form between polymer and surface and less pinning centers (cf. Figure 5). If the polymer contour length is comparable to the thickness increase, the film/air interface roughens too, but the physical reason is very different: the polymers are too short for the equilibrium conformation, and therefore an arbitrary surface conformation is likely.

While it will be difficult to explain these results quantitatively, our finding may provide guidelines to obtain better control when building polyelectrolyte multilayers. Especially, polyelectrolytes which tend to precipitate and form rough multilayers may form smoother multilayers, if the electrostatic forces are promoted at the expense of secondary interactions. This can be achieved by decreasing the temperature (to get away from the precipitation temperature) and by adjusting the pH, the salt, and the salt concentration to make sure that the polyelectrolyte is fully ionized.

Conclusion

Many features of polyelectrolyte multilayers such as thickness per double layer, film/air roughness, or inner interfaces have been investigated in the past as functions of the constituent polyelectrolytes and their side chains.[2] We chose a simpler approach: we varied the adsorption conditions, specifically the counterions, the polymer length, and the temperature. High salt conditions were chosen, to reduce the size and range of electrostatic interactions. Polyelectrolytes precipitate at high temperatures. Since on temperature increase the polymer−solvent interaction increases, more polyelectrolyte adsorbs onto an oppositely charged interface. This idea is verified for PAH/PSS films adsorbed from 1 M KCl aqueous solution at temperatures between 5 and 40 °C approaching the precipitation temperature of PSS at 60 °C. Indeed, the film thickness increases continuously with the adsorption solution temperature; the changes amount to 20−40% (depending on salt conditions). KCl was chosen because thicker films can be formed compared to NaCl or CsCl. Yet if the polyelectrolyte multilayer buildup occurs at elevated temperatures, the electrostatic forces compete with secondary forces during polyelectrolyte adsorption. Since the adsorption/desorption hysteresis is pronounced, an adsorbed polyelectrolyte molecule maintains its conformation and its bonds to the substrate. Therefore, the percentage of strong ion bonds, which serve as pinning centers, decreases. Hence, multilayer buildup is a less robust process, and the film/air interface roughens considerably. Furthermore, UV−vis experiments indicate a structure which is difficult to control on a molecular level.

Acknowledgment. We appreciate discussions with and lab space from Manfred Schmidt. The comments of Michael Cates are appreciated. We thank the DFG (He 1616/7-3,4), the SFB 262 (Project D19), and the BMBF (03C0291C/5) for financial support.

LA011682M